Title

Assessment of Maximum Spinal Deformity in Scoliosis: A Literature Review

Authors and affiliations

Hui-Dong Wu[1,2,3] & Man-Sang Wong[1]

1 Department of Biomedical Engineering, The Hong Kong Polytechnic University, Hong Kong, China

2 Department of Rehabilitation Medicine, West China Hospital, Sichuan University, Chengdu, Sichuan, China

3 Institute for Disaster Management and Reconstruction, Sichuan University-Hong Kong Polytechnic University, Chengdu, Sichuan, China

Address correspondence and reprint requests to Man-Sang Wong, PhD, Department of Biomedical Engineering, The Hong Kong Polytechnic University, Hong Kong, China, Tel: (+852) 27667680; E-mail: m.s.wong@polyu.edu.hk.

Compliance with ethical standards

Funding No funds were received in support of this work.

Conflict of interest Authors declared that they have no conflict of interest.

Abstract

The importance of three-dimensional (3D) assessment of scoliosis has been increasingly recognized. The plane of maximum curvature (PMC), end-apical-end vertebrae plane (EAEP) and best-fit plane (BFP) could assist in reviewing the 3D features of spinal deformities. However, some questions related to PMC, EAEP & BFP have not been thoroughly studied such as (1) any potential differences among them; (2) techniques for obtaining them; (3) and their applications in scoliosis. Therefore, this paper aimed to systematically review the relevant articles to provide useful information for exploring the applications of these 3D descriptors in the clinical assessment and management of scoliosis. This study revealed that BFP could be superior to EAEP and PMC orderly in describing 3D features of a curve segment while it was unknown if the superiority would

be changed or not when BFP or EAEP was simplified in orientation. In addition, the 3D model of the spine or spinal curve reconstructed from the calibrated radiographs or EOS images was the base for the assessment of PMC, EAEP & BFP while the relevant measurements were not studied specifically. Ultrasound technique has also been proposed for the PMC assessment while its measurements are needed to be further investigated. These descriptors have been applied to the 3D assessment, progression monitoring and classification of scoliosis as well as correction evaluation of orthotic and surgical treatments. It is also worthwhile to further explore their clinical applications to better guide the orthotic and surgical strategy making in the future.

Key words: Scoliosis; Maximum deformity; Plane of maximum curvature; End-apical-end vertebrae plane; Best-fit plane

1 Introduction

Scoliosis is complicated three-dimensional (3D) deformity of the spine characterized by lateral curve and axial vertebral rotation (AVR), in which the spine may be shifted/rotated from the sagittal plane to the other anatomical planes.

The coronal Cobb angle measured from the posteroanterior (PA) radiograph is commonly used to assess scoliosis [1-3], however, it may underestimate the severity of spinal curve and could not fully reflect the curve type [4-7]. Therefore, some 3D descriptors were proposed to illustrate the maximum spinal deformity, including the plane of maximum curvature (PMC), end-apical-end vertebrae plane (EAEP) and best-fit plane (BFP), which have been considered to be important in the 3D assessment of scoliosis [8] and increasingly recognized in the orthopedic operation of the spine [9]. However, the difference among these 3D descriptors and which one being superior to the others in describing 3D features of spinal deformity have not been studied. Some techniques have been developed for acquiring these descriptors but no systematic investigation has been done. Although, these 3D descriptors have been applied in assessment [10-14] and 3D classification [8] of scoliosis, their specific role in management of scoliosis was unclear. Thus, this study aimed to systematically review: (1) definitions of PMC, EAEP & BFP; (2) techniques used for obtaining PMC, EAEP & BFP; (3) clinical applications of PMC, EAEP & BFP in scoliosis.

2 Definitions of PMC, EAEP and BFP

As shown in Fig. 1, the PMC is defined as a vertical plane, where a specific region of scoliotic spine (usually bounded by two end vertebrae) is projected onto, presents the maximum spinal curvature by a specified method (e.g. Cobb method) [15]; the EAEP is a plane passing through the centroids of the two end and apical vertebrae of a specific curve [16]; the BFP refers to a plane that best accommodates the vertebrae within a specific curve segment [12,15]. According to the definitions, the orientation of PMC varies along the z axis of the global axis system of the human body [17], recording as PMC-orientation with a corresponding Cobb angle (PMC-Cobb), while the orientation of EAEP and BFP would change along all the x, y and z axes, including EAEP(x)/BFP(x)-, EAEP(y)/BFP(y)- and EAEP(z)/BFP(z)-orientation with corresponding Cobb angles (EAEP(z)/BFP(z)-, EAEP(x)/BFP(x)- and EAEP(y)/BFP(y)-Cobb), respectively. Generally, a “C”

shape curve has a single PMC, EAEP and BFP (Fig. 2) while a "S" shape curve contains two different regional PMCs, EAEPs and BFPs (Fig. 3).

3 Techniques

3.1 Techniques for obtaining PMC

Two main techniques were found to be used for obtaining the PMC, including radiographic and ultrasound techniques. Based on 3D model of the spine or spinal curve reconstructed from the calibrated PA and lateral radiographs or EOS images, the PMC was obtained by rotating a vertical plane along the vertical axis with a certain increment (such as 2.5° [18]) until the maximum spinal curvature was found by the conventional Cobb method [19,20] or computerized Cobb method [5,6,13,14,18,21-29] using automated mathematical techniques [18,21]. Kumar et al. [19] identified the PMC via locating a vertical plane in an orientation matching to the maximum AVR of the specific curve. The sagittal plane served as the reference plane for the PMC-orientation in most studies [5,6,13,18,22,25-27,29].

For the ultrasound technique, the PMC was identified by rotating a vertical plane along the vertical axis to the maximum AVR and confirmed by locating that vertical plane in orientation matching the maximum AVR±2° [30], ±4° [30] and/or ±5° [31] by using the center of laminae (COL) method [32]. The PMC measurements showed high reliability (ICC>0.92 for the PMC-Cobb), and were strongly correlated to those obtained from the EOS system (R^2=0.88 for the PMC-orientation) [30]. The coronal plane was employed as the reference plane for the PMC-orientation [30,31].

3.2 Techniques for obtaining EAEP

Radiographic technique was the main technique for acquiring the EAEP. Based on the 3D reconstruction of the spine or spinal curve, the EAEP could be determined by a triangle plane formed by the connecting lines between the centroids of two end and apical vertebrae of a specific curve (or the end limits and apex of a curve) [7,11,10,33,34].

The da Vinci representation was a useful method to present the EAEP in the top view [7,8] by projecting the centroids of the end and apical vertebrae (or the end limits and apex) of a specific curve onto the transverse plane, and the track of the EAEP appeared in a triangle. By contrast, the simplified da Vinci representation, which replaced the triangle with an arrow emitting originally from the central hip vertical axis (CHVA) to the track of apex on the transverse plane [7,8]. The direction of the arrow represented the EAEP(z)-orientation, and the length of the arrow was proportional to the EAEP(z)-Cobb. For ensuring reasonable variables for analysis, only the EAEP(z)-orientation was considered in most studies [7,8,11,35,36].

3.3 Techniques for obtaining BFP

Based on the 3D reconstruction of the spine or spinal curve using the radiographic technique, BFP could be determined by minimizing the sum of square linear distances [14] or linear distances [12,33] from the centroids of the vertebrae within the spinal curve to that unknown plane. The number of BFP existing in a scoliotic spine could be determined by linear fitting coefficient, the maximum normal distance from the centroids of the vertebrae to that plane [12]. If the coefficient is smaller than or equal to a certain value such as10mm, one unique global BFP is determined; otherwise, regional BFPs exist [12]. Some studies identified the BFP by isolating vertebrae within the curve and establishing a plane in which the isolated vertebrae showed unique flexion [37-39]. For ensuring reasonable variables, the BFP-orientation was simplified in some studies, keeping only BFP(z)-orientation [12] or BFP(z)/BFP(x)-orientation [14,33].

4 Applications of PMC, EAEP and BFP in scoliosis

4.1 Applications in 3D assessment, progression monitoring and classification of scoliosis

There are interdependent relationships between these 3D descriptors and the Cobb angle in the coronal and sagittal planes. The PMC/BFP(z)-Cobb was generally 1°-6° greater than the coronal Cobb angle [29-31,37,40-42] as shown in Table 1, but no significant correlation was observed [11].

Table 1 Comparison of average coronal Cobb and PMC/BFP(z)-Cobb

	Coronal Cobb angle (°)	PMC/BFP(z)-Cobb (°)	Difference (°)
Sawatzky et al. [37]	57	58^	1
Delorme et al. [40]	51	55#	4
Villemure et al. [41]	35	39#	4
Vo et al. [31]	23	27#	4
Trac et al. [30]	25	26#	1
Labelle et al. [29]	35	40#	5
Carpineta et al. [42]	48	54#	6

Difference = PMC/BFP(z)-Cobb – coronal Cobb

#: PMC-Cobb

^: BFP(z)-Cobb

The PMC-orientation was found to have progression in 71% subjects with adolescent idiopathic scoliosis (AIS) during an observation period of 22.8±10.8 months [5]. It was significantly higher in the progressive than in the non-progressive AIS at the initial visit (mean difference (MD)=12.1°) [20] and could increase with the severity of spinal deformities [5,20].

The PMC, EAEP & BFP have been proposed for the 3D classification of scoliosis. The Lenke type-1 could be split into different sub-types based on the PMC [13,14], EAEP [7,11,36,43] or BFP [14]. The EAEP(z)-orientation had superiority to other clinical indices (e.g. kyphosis, lordosis, corona Cobb angle and AVR) in differentiating sub-types within all the Lenk types [36,43]. Furthermore, the BFP(z)/(x)-orientation [14] and EAEP(z)-orientation [43] could be superior to the PMC-orientation in subclassifying the Lenke type-1. Additionally, it was worthwhile to note that the clustering algorithm could be applied when refining the Lenke types using the PMC [13,14] or EAEP [7,36,44,43].

4.2 Applications in effectiveness evaluation of surgical and orthotic treatments

The correction of surgical treatment was 24%-51% in PMC-Cobb [6,23], and 19%-73% but mostly 25%-41% in PMC-orientation [6,23,26,27]. By contrast, the correction in coronal Cobb angle was slightly higher (50% versus 24% [23] and 49%-65% versus 32%-51% [6]). The correction in BFP(z)-orientation was 57%-62%

[37,38]. However, a loss of 30% and 25% in correction was observed in the PMC-orientation and coronal Cobb angle respectively in a follow-up study of 2.5 years [26].

Two studies referred to the application of the PMC in 3D correction evaluation of Boston orthosis for patients with AIS. Similar correlation in the PMC-Cobb and coronal Cobb angle was found, with 17%-39% and 17%-33%, respectively. However, significant correction of the PMC-orientation (38%) was only observed for lumbar curves provided by orthosis designed and adjusted with a computer-assisted tool [29]. Within the orthosis, the PMC-orientation of the thoracic curves tended not to change or even increased [24,29].

5 Discussion

5.1 Definitions of PMC, EAEP and BFP

In a normal spine, as all the spinal curves (physiological curves) lie in the sagittal plane, there is usually one unique global PMC, EAEP & BFP, which all overlap with the sagittal plane. However, in a scoliotic spine, there might be one unique global but mostly several regional PMCs, EAEPs & BFPs connected at their adjacent zones [8,12,33], presenting notably different Cobb angles and/or orientations. The PMC, EAEP & BFP take two end-vertebrae, two end-vertebrae and an apical vertebra, and all the vertebrae within the curve into account correspondingly. Thus, the BFP may have more potential to reflect the 3D feature of a curve segment and followed by the EAEP and PMC orderly. From a practical and reasonable point of view, most studies only took EAEP(z)/BFP(z)-orientation [7,11,12,35,36] or BFP(z)/(x)-orientation [14,33] into consideration. The BFP(z)- [14] and EAEP(z)-orientation [43] were reported to be superior to the PMC-orientation in subcategorizing the Lenk type-1, but further studies were needed to have a comprehensive understanding of their superiority in classification of scoliosis.

5.2 Techniques for obtaining PMC, EAEP and BFP

The 3D reconstruction of spine or spinal curve was the base for the assessment of PMC, EAEP & BFP. The accuracy and reproducibility of the 3D reconstruction were demonstrated in most studies [28,37,45-50]. However, the reliability and validity of the PMC, EAEP & BFP measurements were rarely investigated specially, except a few reports related to the variability of PMC measurements (MD=0.7°-1.6° for the PMC-

Cobb, and MD=1.5°-2.7° and root-mean-square=6.0°-14.0°/9.3°-20.4° for the PMC-orientation [28,49]). This could be lacking a gold standard. Computed tomography (CT) and magnetic resonance imaging (MRI) are commonly used for 3D assessment of scoliosis but not commonly applied to the assessment of the PMC, EAEP & BFP. Besides, the recumbent position used in CT/MRI limits their use for validating these descriptors' measurements acquired in standing position. There existed relationships between the 3 descriptors and the Cobb angle (in the coronal and sagittal planes) [7,18,43], and between the coronal and sagittal Cobb angles (in the standing and recumbent positions) [51]. These relationships may provide a link to validate the standing PMC, EAEP & BFP measurements with those obtained from CT/MRI in the recumbent position indirectly.

Several points should be noted. Firstly, the da Vinci representation [7,8] provides a very intuitional vision for the orientation of EAEP from the top view, but it, especially after being simplified, remains only EAEP(z)-orientation while missing EAEP(x)/(y)-orientation. Thus, the EAEP presented in the simplified da Vinci representation could be interpreted as a vertical plane passing though the CHVA and the apical vertebra. Secondly, the computerized Cobb method used for the PMC/EAEP/BFP-Cobb measurement was found slightly overestimated the coronal Cobb angle by 11%-12% as compared to the conventional Cobb method [52] while the difference between the PMC/EAEP/BFP-Cobbs acquired using the computerized and conventional Cobb methods needed further investigation. This difference may be due to that the computerized was based on the two lines perpendicular to the spinal curve at its inflection points [18,21] while the conventional was based on the two lines parallel to the endplates of the two end vertebrae. Additionally, the sagittal plane served as the reference of the PMC/EAEP(z)/BFP(z)-orientation in most studies [5,6,13,18,22,25-27,29]. The possible reason could be the original PMC/EAEP(z)/BFP(z) lies in the sagittal plane with an orientation of 0° in a normal spine and with a certain orientation in a scoliotic spine.

The ultrasound technique is characterized by radiation-free and user-friendly. It has been demonstrated to be reliable and accurate for the assessment of spinal lateral curvature [53-57] and AVR [58-60], and used for assessing the spinal flexibility [61-64] and curve progression [65] as well as the spinal orthosis casting [66] and fitting [67]. In a study of Trac et al. [30], the PMC measurements obtained using the ultrasound technique

were very reliable (ICC>0.92), and also strongly correlated to those obtained from the EOS system (R^2=0.88). Besides, it allows the patients to lie in a recumbent position [57] which makes it possible to compare with the CT/MRI in PMC acquisition. With these advantages, ultrasound technique may be a promising tool for the 3D assessment of scoliosis.

5.3 Applications

The PMC/EAEP/BFP-Cobb and -orientation reveal the "true" curvature and the degree of a curve segment being shifted/rotated towards the coronal plane, respectively. There are interdependent relationships between the PMC, EAEP & BFP and Cobb angles in the coronal and sagittal planes [7,10-12,18,22,43], and the latters can be considered as the components of the formers. For the same PMC/EAEP/BFP-orientation, a greater (or smaller) PMC/EAEP(z)/BFP(z)-Cobb could result in greater (or smaller) coronal and sagittal Cobb angles, and for the same PMC/EAEP/BFP-Cobb, a greater (or smaller) PMC/EAEP(z)/BFP(z)-orientation with respect to the sagittal plane could cause a greater (or smaller) Cobb angle in the coronal plane but a smaller (or greater) Cobb angle in the sagittal plane. The coronal Cobb angle was found 1°-6° lower in magnitude as compared to the PMC/BFP(z)-Cobb [29-31,37,40-42]. This may imply that a patient who has progression ≤5° or curve ≤45° based on the coronal Cobb angle may have progression ≥6° or curve > 45° when using the PMC/BFP(z)-Cobb. As progression≤5° or curve≤45° is a crucial standard to assess the success of treatments [68], thus, in this case, the treatment may be misjudged as success and the clinicians may miss an optimal time to review the relevant treatment strategy. From this point of view, PMC/EAEP/BFP may provide clinically significant information for the assessment and management of scoliosis.

Because of the interdependent relationships, any progression in the coronal and sagittal Cobb angles could result the progression in the PMC [5,69]. The finding that PMC-orientation was higher in the progressive AIS could be employed as a factor for differentiating the progressive and nonprogressive AIS [5,20].

The first classification system of scoliosis, which was known as King's system, was presented in 1950s but only for thoracic scoliosis [70], and several classification systems were proposed subsequently. In 1997, the Lenke classification system was introduced with both the thoracic and (thoraco)lumbar scoliosis taken into

consideration [71]. However, in these systems, there is a common limitation that only the coronal (and sagittal) radiograph(s) was(were) considered. In a normal spine, the spinal curve lies in the sagittal plane but in a scoliotic spine, it may shift/rotate towards the coronal plane. The coronal and sagittal curvature may be the components of and may not always be corresponding to the "true" spinal curvature, as exemplified previously that two remarkably different curves could have the same coronal Cobb angle value [7,8]. The Lenke types, which are usually used in orthotic and surgical planning, could be subclassified into different sub-types, such as the Lenke type-1 curves based on the PMC [13,14], EAEP [7,8,11,36,43] or BFP [14]. Different curve sub-types may require different orthotic or surgical strategies; hence, it may be necessary to take the PMC, EAEP or EFP as a useful reference when differentiating the curve types. Regarding to the superiority of PMC, EAEP & BFP in identifying curve types, both the BFP(z)/(x)-orientation [14] and EAEP(z)-orientation [43] appeared to be superior to the PMC-orientation for the Lenke type-1 while further investigation is needed to understand whether the superiority exists in other Lenke types to facilitate a comprehensive classification of scoliosis. In additional, when refining the 3D classification of scoliosis, the cluster analysis of 3D shape of spine was applied [7,13,14,36,43], which allowed automatic classification and could also identify the differences between patients not evident in two-dimensional radiographs. Thus, the cluster analysis could be an option when differentiating the curve types of scoliosis.

The 3D correction of scoliosis via surgical treatment has been demonstrated, including correction in the curve magnitude (PMC-Cobb and coronal Cobb angle) [6,23] and rotation of curve segment (PMC/BFP(z)-orientation) [6,23,26,27,37,38]. It is generally noted that the correction in the coronal Cobb angle was higher than the PMC-Cobb and its possible reason may be the correction in the coronal Cobb angle resulted from a combined effect of reduction in the "true" curve magnitude and rotation of the curve segment. Additionally, there was a degree of loss in correction within a period of average 2.5 years [26], thus, the effectiveness of surgical treatment should be followed up at a long-term basis.

Only two studies referred to the 3D correction evaluation of orthotic treatment (Boston orthosis) based on the PMC. Significant correction in the PMC-Cobb and coronal Cobb angle were observed for both the thoracic and lumbar curves, however, only the correction of PMC-orientation of the lumbar curves was

documented for the Boston orthosis designed and adjusted via computer-assisted tool [29]. For the thoracic curves, the PMC-orientation tended not to change or even increased after wearing orthosis [24,29], indicating that the thoracic curves stayed in the deformed position or shifted/rotated towards the coronal plane even more after orthosis application. In this case, the coronal Cobb angle alone may not be comprehensive enough to reflect the "true" correction of scoliosis, and it may be necessary to include PMC, EAEP and BFP as useful references.

6 Conclusion

This review suggested that the BFP would be superior to the EAEP and PMC in the description of maximum spinal deformity, however, the priority of application among these 3D descriptors should be further explored. These 3D descriptors could be obtained using radiographic technique, while the reliability and/or validity of the relevant measurements need further investigation. Besides, ultrasound technique is another option for acquiring the PMC but its properties (reliability & validity) require more evaluation. The importance of the PMC, EAEP & BFP for scoliosis in 3D assessment, classification, monitoring and evaluation of surgical and orthotic treatments has been demonstrated. It is also worthwhile to gather the information of these 3D descriptors to better guide the formation of strategy for orthotic and surgical interventions in the future.

Captions

Fig. 1 Scoliotic curve: a) plane of maximum curvature, b) end-apical-end vertebrae plane and c) best-fit plane

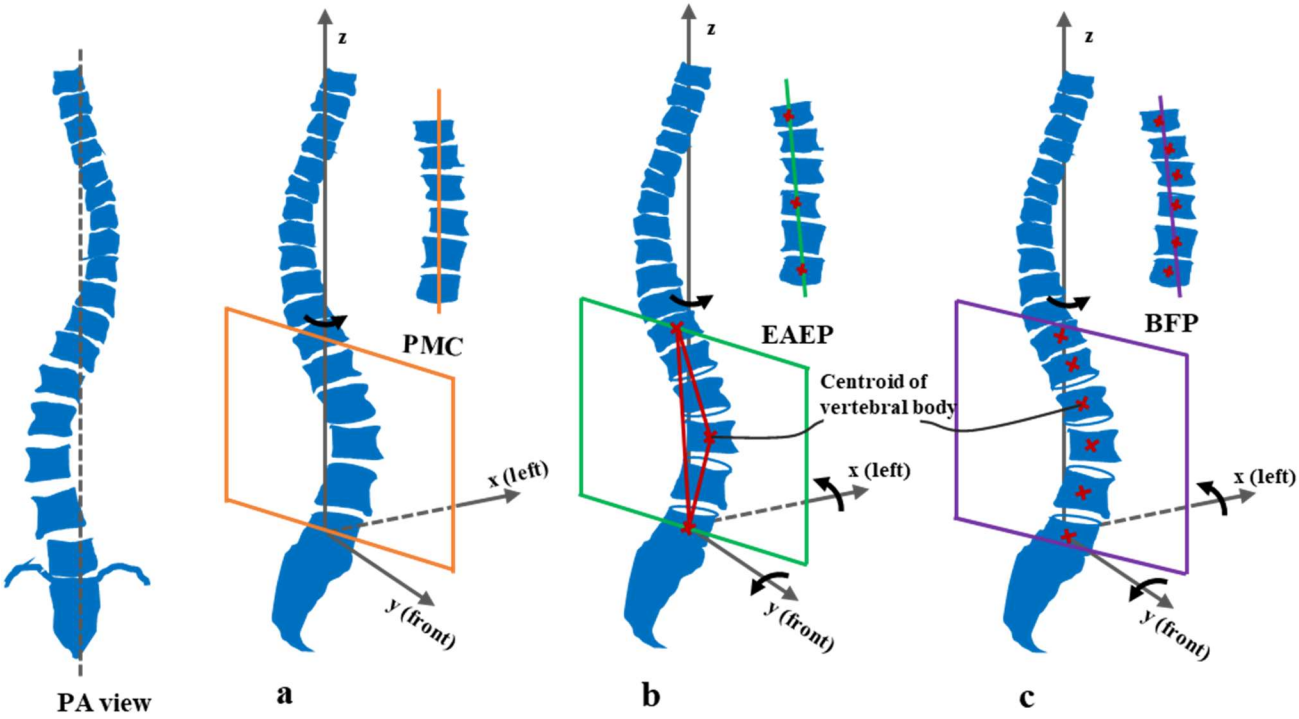

Fig. 2 In a "C" shape curve, there is one plane of maximum curvature, end-apical-end vertebrae plane, and best-fit plane

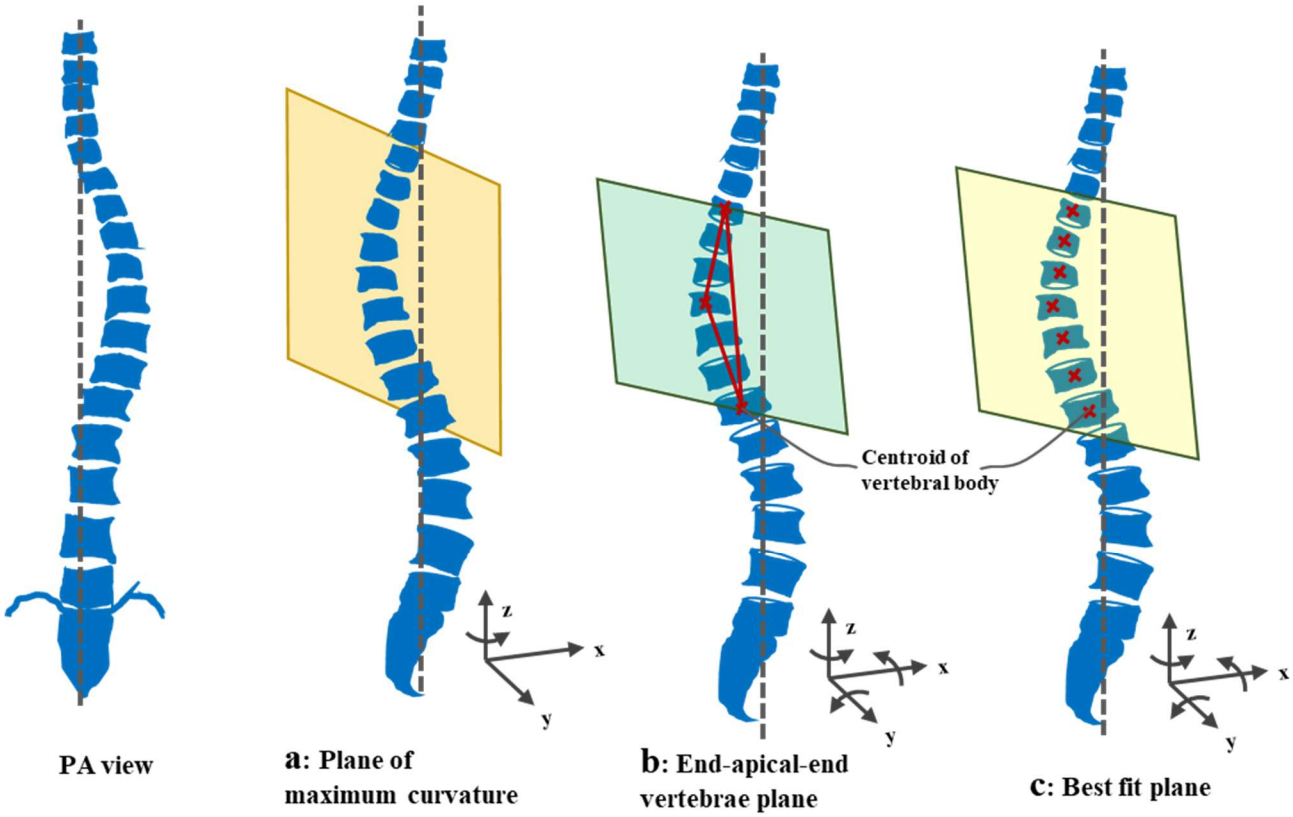

Fig. 3 In a "S" shape curve, there are two different regional planes of maximum curvature, end-apical-end vertebrae planes, and best-fit planes

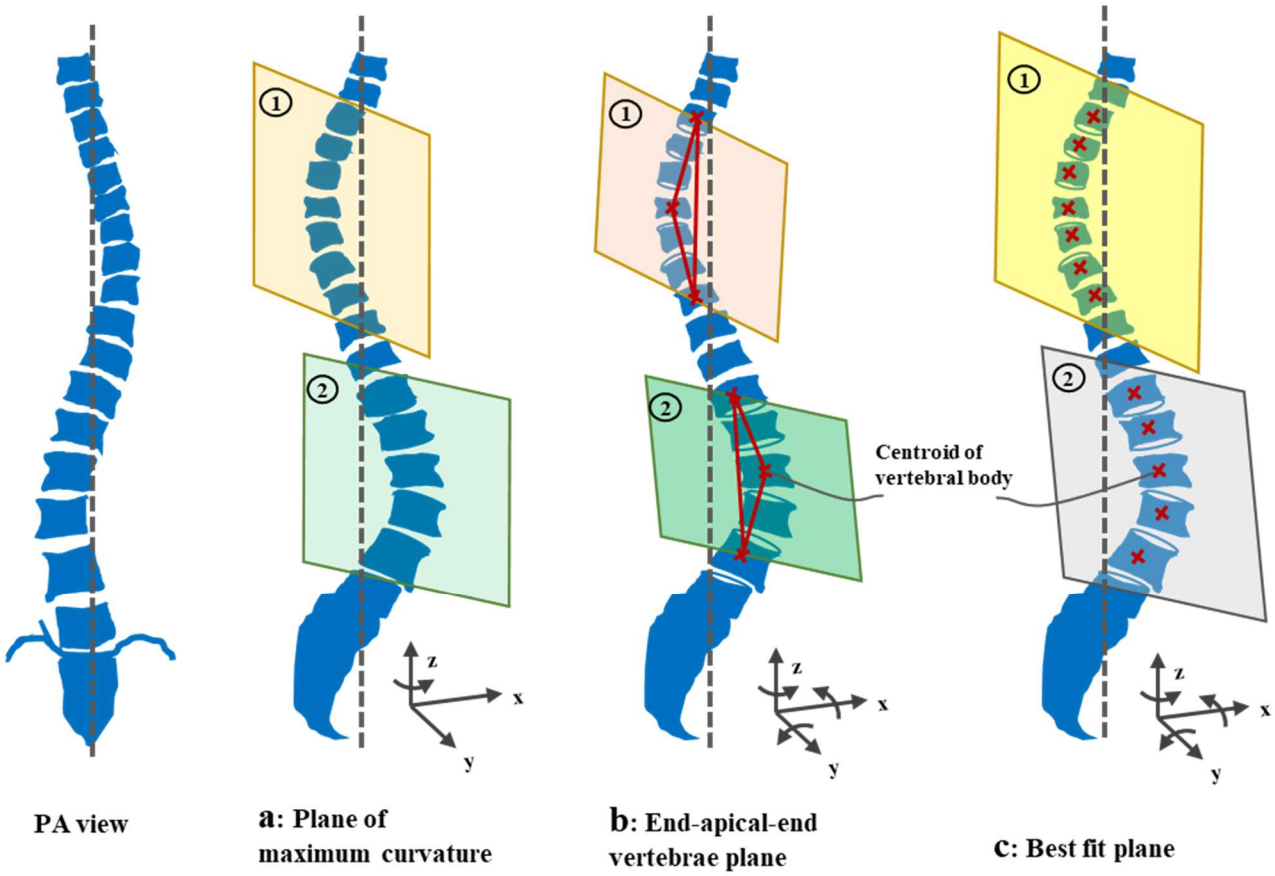

References

1. Wright N. (2000). Imaging in scoliosis. *Archives of Dissease Childhood*, 82(1), 38-40.

2. Kotwicki T. (2008). Evaluation of scoliosis today: examination, x-rays and beyond. *Disability and Rehabilitation*, 30(10), 742-751.

3. Kotwicki T., Negrini S., Grivas T.B., Rigo M., Maruyama T., Durmala J., Zaina F. (2009). Methodology of evaluation of morphology of the spine and the trunk in idiopathic scoliosis and other spinal deformities - 6th SOSORT consensus paper. *Scoliosis and Spinal Disorders*, 4(1), 1-16.

4. Lindahl O., Movin A. (1968). Measurement of the deformity in scoliosis. *Acta Orthopaedica Scandinavica*, 39(3), 291-302.

5. Villemure I., Aubin C.E., Grimard G., Dansereau J., Labelle H. (2001). Progression of vertebral and spinal three-dimensional deformities in adolescent idiopathic scoliosis: a longitudinal study. *Spine*, 26(20), 2244-2250.

6. Delorme S., Labelle H., Aubin C.E., de Guise J.A., Rivard C.H., Poitras B., Dansereau J. (2000). A three-dimensional radiographic comparison of Cotrel–Dubousset and Colorado instrumentations for the correction of idiopathic scoliosis. *Spine*, 25(2), 205-210.

7. Sangole A.P., Aubin C.E., Labelle H., Stokes I.A., Lenke L.G., Jackson R., Newton P. (2008). Three-dimensional classification of thoracic scoliotic curves. *Spine*, 34(1), 91-99.

8. Labelle H., Aubin C.E., Jackson R., Lenke L., Newton P., Parent S. (2011). Seeing the Spine in 3D: How Will It Change What We Do? *Journal of Pediatric Orthopaedics*, 31(1), S37-S45.

9. Lenke L.G. (2012). What's new in the surgical care of adolescent idiopathic scoliosis (AIS). *ArgoSpine News & Journal*, 24(1-2), 62-66.

10. Pasha S., Cahill P.J., Dormans J.P., Flynn J.M. (2016). Characterizing the differences between the 2D and 3D measurements of spine in adolescent idiopathic scoliosis. *European Spine Journal*, 25(10), 3137-3145.

11. Bernard J.C., Berthonnaud E., Deceuninck J., Journoud-Rozand L., Notin G., Chaleat-Valayer E. (2018). Three-dimensional reconstructions of Lenke 1A curves. *Scoliosis and Spinal Disorders*, 13, 5.

12. Berthonnaud E., Dimnet J., Hilmi R. (2009). Classification of pelvic and spinal postural patterns in upright position. specific cases of scoliotic patients. *Computerized Medical Imaging and Graphics*, 33(8), 634-643.
13. Kadoury S., Labelle H. (2012). Classification of three-dimensional thoracic deformities in adolescent idiopathic scoliosis from a multivariate analysis. *European Spine Journal*, 21(1), 40-49.
14. Duong L., Mac-Thiong J.M., Cheriet F., Labelle H. (2009). Three-dimensional subclassification of Lenke type 1 scoliotic curves. *Journal of Spinal Disorders & Techniques*, 22(2), 135-143.
15. Stokes I.A.F (1994). Three-dimensional terminology of spinal deformity: a report presented to the scoliosis research society by the scoliosis research society working group on 3-D terminology of spinal Deformity. *Spine*, 19(2), 236-248.
16. Perdriolle R., Borgne P.L., Dansereau J., Guise J., Labelle H. (2001). Idiopathic scoliosis in three dimensions: a succession of two-dimensional deformities? *Spine*, 26(24), 2719–2726.
17. Sangole A., Aubin C., Labelle H., Lenke L., Jackson R., Newton P., Stokes I. (2010). The central hip vertical axis: a reference axis for the scoliosis research society three-dimensional classification of idiopathic scoliosis. *Spine*, 35(12), E530-E534.
18. Stokes I.A.F., Bigalow L.C., Moreland M.S. (1987). Three-dimensional spinal curvature in idiopathic scoliosis. *Journal of Orthopaedic Research*, 5(1), 102-113.
19. Kumar S., Nayak K.P., Hareesha K.S. (2017). Quantification of spinal deformities using combined SCP and geometric 3D reconstruction. *Biomedical Signal Processing and Control*, 31,181-188.
20. Nault M.L., Mac-Thiong J.M., Roy-Beaudry M., Turgeon I., Deguise J., Labelle H., Parent S. (2014). Three-dimensional spinal morphology can differentiate between progressive and nonprogressive patients with adolescent idiopathic scoliosis at the initial presentation: a prospective study. *Spine*, 39(10), E601-606.
21. Labelle H., Dansereau J., Bellefleur C., Jequier J.C. (1995). Variability of geometric measurements from three-dimensional reconstructions of scoliotic spines and rib cages. *European Spine Journal*, 4(2), 88-94.
22. Stokes I.A.F. (1989). Axial rotation component of thoracic scoliosis. *Journal of Orthopaedic Research*, 7(5), 702-708.

23. Labelle H., Dansereau J., Bellefleur C., Poitras B., Rivard C.H., Stokes I.A., de Guise J. (1995). Comparison between preoperative and postoperative three-dimensional reconstructions of idiopathic scoliosis with the Cotrel-dubousset procedure. *Spine*, 20(23), 2487-2492.

24. Labelle H., Dansereau J., Bellefleur C., Poitras B. (1996). Three-dimensional effect of the Boston brace on the thoracic spine and rib cage. *Spine*, 21(1), 59-64.

25. Delorme S., Labelle H., Aubin C.E., de Guise J.A., Rivard C.H., Poitras B., Coillard C., Dansereau J. (1999). Intraoperative comparison of two instrumentation techniques for the correction of adolescent idiopathic scoliosis: rod rotation and translation. *Spine*, 24(19), 2011-2011.

26. Papin P., Labelle H., Delorme S., Aubin C.E., de Guise J.A., Dansereau J. (1999). Long-term three-dimensional changes of the spine after posterior spinal instrumentation and fusion in adolescent idiopathic scoliosis. *European Spine Journal*, 8(1), 16-21.

27. Delorme S., Labelle H., Poitras B., Rivard C.H., Coillard C., Dansereau J. (2000). Pre-, intra-, and postoperative three-dimensional evaluation of adolescent idiopathic scoliosis. *Journal Spinal Disorders*, 13(2), 93-101.

28. Moura D.C., Boisvert J., Barbosa J.G., Labelle H., Tavares J.M. (2011). Fast 3D reconstruction of the spine from biplanar radiographs using a deformable articulated model. *Medical Engineering & Physics*, 33(8), 924-933.

29. Labelle H., Bellefleur C., Joncas J., Aubin C.E., Cheriet F. (2007). Preliminary evaluation of a computer-assisted tool for the design and adjustment of braces in idiopathic scoliosis: a prospective and randomized study. *Spine*, 32(8), 835-884.

30. Trac S., Zheng R., Hill D.L., Lou E. (2019). Intra- and interrater reliability of Cobb angle measurements on the plane of maximum curvature using ultrasound imaging method. *Spine Deformity*, 7(1), 18-26.

31. Vo Q.N., Lou E.H.M., Le L.H. (2015). 3D ultrasound imaging method to assess the true spinal deformity. In: *37th Annual International Conference of the IEEE Engineering in Medicine and Biology Society*, pp. 1540e3.

32. Chen W., Lou E.H., Zhang P.Q., Le L.H., Hill D. (2013). Reliability of assessing the coronal curvature of children with scoliosis by using ultrasound images. *Journal of Childrens Orthopaedics*, 7(6), 521-529.

33. Berthonnaud E., Hilmi R., Dimnet J. (2012). Geometric structure of 3D spinal curves: plane regions and connecting zones. *ISRN Orthopedics*, 2012, 1-10.

34. Berthonnaud E., Papin P., Deceuninck J., Hilmi R., Bernard J.C., Dimnet J. (2016). The use of a photogrammetric method for the three-dimensional evaluation of spinal correction in scoliosis. *International Orthopaedics*, 40(6), 1187-1196.

35. Kohashi Y., Oga M., Sugioka Y. (1996). A new method using top views of the spine to predict the progression of curves in idiopathic scoliosis during growth. *Spine*, 21(2), 212-217.

36. Thong W., Parent S., Wu J., Aubin C., Labelle H., Kadoury S. (2016). Three-dimensional morphology study of surgical adolescent idiopathic scoliosis patient from encoded geometric models. *European Spine Journal*, 25(10), 3104-3113.

37. Sawatzky B., Tredwell S.J., Jang S.B., Black A.H. (1998). Effects of three-dimensional assessment on surgical correction and on hook strategies in multi-hook instrumentation for adolescent idiopathic scoliosis. *Spine*, 23(2), 201-205.

38. Stephen T.J., Bonita S.J., Barbara H.L. (1999). Rotations of a helix as a model for correction of the scoliotic spine. *Spine*, 24(12), 1223-1227.

39. Sawatzky B.J., Jang S.B., Tredwell S.J., Black A., Reilly C.W., Booth K.S. (1998). Intra-operative analysis of scoliosis surgery in 3-D. *Computer Methods in Biomechanics and Biomedical Engineering*, 1(3), 211-221.

40. Delorme A.S., Labelle H.,Aubin C.E.,De Guise J.A., Jacques, Rivard A, Charles-H. , Poitras A, Benoît, Dansereau A, Jean (2000). A Three-Dimensional Radiographic Comparison of Cotrel–Dubousset and Colorado Instrumentations for the Correction of Idiopathic Scoliosis. *Spine*, 25(2), 205-205.

41. Villemure I., Aubin C., Grimard G., Dansereau J., Labelle H. (2001). Progression of vertebral and spinal three-dimensional deformities in adolescent idiopathic scoliosis - a longitudinal study. *Spine*, 26(20), 2244-2250.

42. Carpineta L., Labelle H. (2003). Evidence of three-dimensional variability in scoliotic curves. *Clinical Orthopaedics and Related Research*, 412(139-148.

43. Stokes I.A.F., Sangole A.P., Aubin C.E. (2009). Classification of scoliosis deformity three-dimensional spinal shape by cluster analysis. *Spine*, 34(6), 584-590.

44. Shen J., Kadoury S., Labelle H., Roy-Beaudry M., Aubin C.E., Parent S. (2017). Geometric torsion in adolescent idiopathic scoliosis: a new method to differentiate between Lenke 1 subtypes. *Spine*, 42(9), E532-E538.

45. Humbert L., Guise J.A.D., Aubert B., Godbout B., Skalli W. (2009). 3D reconstruction of the spine from biplanar x-rays using parametric models based on transversal and longitudinal inferences. *Medical Engineering & Physics*, 31(6), 681-687.

46. Kadoury S., Cheriet F., Labelle H. (2009). Personalized x-ray 3-D reconstruction of the scoliotic spine from hybrid statistical and image-based models. *IEEE Transactions on Medical Imaging*, 28(9), 1422-1435.

47. Kadoury S., Cheriet F., Laporte C., Labelle H. (2007). A versatile 3D reconstruction system of the spine and pelvis for clinical assessment of spinal deformities. *Medical & Biological Engineering & Computing*, 45(6), 591-602.

48. Kadoury S., Cheriet F., Dansereau J., Labelle H. (2007). Three-dimensional reconstruction of the scoliotic spine and pelvis from uncalibrated biplanar x-ray images. *Journal of Spinal Disorders & Techniques*, 20(2), 160-168.

49. Delorme S., Petit Y., de Guise J.A., Labelle H., Aubin C.E., Dansereau J. (2003). Assessment of the 3-d reconstruction and high-resolution geometrical modeling of the human skeletal trunk from 2-D radiographic images. *IEEE Transactions on Biomedical Engineering*, 50(8), 989-998.

50. Cheriet F., Dansereau J., Petit Y., Aubin C.E., Labelle H., Au De Guise **J.** (1999). Towards the self-calibration of a multi-view radiographic imaging system for the 3D reconstruction of the human spine and rib cage. *International Journal of Pattern Recognition and Artificial Intelligence*, 13(5), 761-779.

51. Wessberg P., Danielson B.I**.,** Wille´n J. (2006). Comparison of Cobb angles in idiopathic scoliosis on standing radiographs and supine axially loaded MRI. *Spine*, 31(26), 3039–3044.

52. Stokes I.A.F, Shuma-Hartswick D., Moreland M.S. (1988). Spine and back-shape changes in scoliosis. *Acta Orthopaedica Scandinavica*, 59(2), 128-133.

53. Zheng Y.P., Lee T.T.Y., Lai K.K.L., Yip B.H.K., Zhou G.Q., Jiang W.W., Cheung J.C.W., Wong M.S., Ng B.K.W., Cheng J.C.Y., Lam T.P. (2016). A reliability and validity study for Scolioscan: a radiation-free scoliosis assessment system using 3D ultrasound imaging. *Scoliosis and Spinal Disorders*, 11(1), 1-15.

54. Zheng R., Chan A.C., Chen W., Hill D.L., Le L.H., Hedden D., Moreau M., Mahood J., Southon S., Lou E. (2015). Intra- and inter-rater reliability of coronal curvature measurement for adolescent idiopathic scoliosis using ultrasonic imaging method - A pilot study. *Spine Deformity*, 3(2), 151-158.

55. Young M., Hill D.L., Zheng R., Lou E. (2015). Reliability and accuracy of ultrasound measurements with and without the aid of previous radiographs in adolescent idiopathic scoliosis (AIS). *European Spine Journal*, 24(7), 1427-1433.

56. Brink R.C., Wijdicks S.P.J., Schlösser T.P., Kruyt M.C., Beek F.J.A., Castelein R.M., Tromp I.N. (2018). A reliability and validity study for different coronal angles using ultrasound imaging in adolescent idiopathic scoliosis. *Spine journal*, 18(6), 979-985.

57. Wang Q., Li M., Lou E.H.M., Wong M.S. (2015). Reliability and validity study of clinical ultrasound imaging on lateral curvature of adolescent idiopathic scoliosis. *PLoS One*, 10(8), e0135264.

58. Chen W., Le L.H., Lou E.H. (2016). Reliability of the axial vertebral rotation measurements of adolescent idiopathic scoliosis using the center of lamina method on ultrasound images: in vitro and in vivo study. *European Spine Journal*, 25(10), 3265-3273.

59. Chen W., Lou E., Le L.H. (2015). A reliable semi-automatic program to measure the vertebral rotation using the center of lamina for adolescent idiopathic scoliosis. In: *37th Annual International Conference of the IEEE Engineering in Medicine and Biology Society,* pp.159-162.

60. Wang Q., Li M., Lou E.H., Chu W.C., Lam T.P., Cheng J.C., Wong M.S. (2016). Validity study of vertebral rotation measurement using 3-D ultrasound in adolescent idiopathic scoliosis. *Ultrasound in Medicine and Biology*, 42(7), 1473-1481.

61. Zheng R., Hill D., Hedden D., Moreau M., Le L.H., Raso J., Lou E. (2017). Assessment of curve flexibility on scoliotic surgical candidates using ultrasound imaging method. *Ultrasound in Medicine and Biology*, 43(5), 934-942.

62. Khodaei M., Hill D., Zheng R., Le L.H., Lou E.H.M. (2018). Intra- and inter-rater reliability of spinal flexibility measurements using ultrasonic (US) images for non-surgical candidates with adolescent Idiopathic scoliosis: a pilot study. *European Spine Journal*, 27(9), 2156-2164.

63. He C., To M.K., Cheung J.P., Cheung K.M., Chan C.K., Jiang W.W., Zhou G.Q., Lai K.K., Zheng Y.P., Wong M.S. (2017). An effective assessment method of spinal fexibility to predict the initial in-orthosis correction on the patients with adolescent idiopathic scoliosis (AIS). *PLoS One*, 12(12), e0190141-.

64. Lou E., Zheng R., Le L., Hill D., Raso J., Hedden D., Mahood J., Moreau M. (2015). Curve flexibility assessment on AIS surgical candidates using ultrasonic imaging method - a preliminary study. *Scoliosis*, 10(Suppl 1), O39.

65. Zheng R., Hill D., Hedden D., Moreau M., Southon S., Lou E. (2018). Assessment of curve progression on children with idiopathic scoliosis using ultrasound imaging method. *European Spine Journal*, 27(5), 1-6.

66. Lou E., Chan A., Donauer A., Tilburn M., Hill D. (2015). Ultrasound-assisted brace casting for adolescent idiopathic scoliosis. *Scoliosis*, 10(Suppl 1), O38.

67. Li M., Ng B., Cheng J., Ying M., Zheng Y.P., Lam T.P., Wong W.Y., Wong M.S. (2012). Could clinical ultrasound improve the fitting of spinal orthosis for the patients with AIS? *European Spine Journal*, 21(10), 1926-1935.

68. Negrini S., Donzelli S., Aulisa A.G., Czaprowski D., Schreiber S., de Mauroy J.C**.,** et al. (2018). 2016 SOSORT guidelines: orthopaedic and rehabilitation treatment of idiopathic scoliosis during growth. *Scoliosis and Spinal Disorders*, 13, 3.

69. Deacon P., Flood B.M., Dickson R.A. (1984). Idiopathic scoliosis in three dimensions: a radiographic and morphometric analysis. *Journal of Bone and Joint Surgery-British Volume*, 66(4), 509-512.

70. Ponseti I., Friedman B. (1950). Prognosis in idiopathic scoliosis. *Journal of Bone and Joint Surgery-American Volume*, 32A(2), 381-395.

71. King H., Moe J., Bradford D, Winter R (1983). The selection of fusion levels in thoracic idiopathic scoliosis. *Journal of Bone and Joint Surgery-American Volume*, 65(9), 1302-1313.